ChemComm

RSC Publishing

COMMUNICATION

View Article Online
View Journal | View Issue

Cite this: *Chem. Commun.*, 2013, **49**, 5742

Received 24th January 2013,
Accepted 1st May 2013

DOI: 10.1039/c3cc40599k

www.rsc.org/chemcomm

Electrochemical synthesis of p-type Zn-doped α-Fe_2O_3 nanotube arrays for photoelectrochemical water splitting†

Xiaopeng Qi,[ab] Guangwei She,*[a] Meng Wang,[ab] Lixuan Mu[a] and Wensheng Shi*[a]

A facile electrochemical method is developed to synthesize p-type Zn-doped α-Fe_2O_3 nanotube arrays that demonstrate excellent photoelectrochemical properties for water splitting.

Photoelectrochemical water splitting represents an ingenious solution to the energy crisis and environmental issues by utilizing semiconductors to harvest solar energy and store it as a clean fuel, H_2.[1] Narrow band-gap semiconductors hold great promise in absorbing visible light but generally suffer from improper energy band positions and insufficient photovoltages, therefore requiring external voltages to assist the overall water splitting reaction. Recently, p–n junction photoelectrodes and tandem cells have emerged as attractive designs to overcome these drawbacks.[2] In most of these devices, p-type semiconductors are required either to form p–n junctions to increase the photovoltages or to serve as photocathodes responsible for the water reduction half reaction.[2] Among the p-type candidates, such as p-Si, Cu_2O and InP,[3] α-Fe_2O_3 stands out due to its ideal bandgap of 2.0–2.2 eV, abundance, non-toxicity and stability.[4] Although inherent α-Fe_2O_3 is an n-type semiconductor due to the oxygen vacancy,[5] p-type α-Fe_2O_3 is attainable through proper doping with impurities such as Zn, Cu, Mg or N.[2a,e,6] Moreover, the dopants could modify the conduction band position of α-Fe_2O_3, thus satisfying the thermodynamic requirements for water splitting.[6a,b]

Although promising, α-Fe_2O_3 suffers from inefficient charge collection,[4] which could result from its the poor conductivity,[7] short photogenerated carrier lifetime,[8] and short carrier diffusion length as compared to its long light penetrating length.[4] In this regard, a nanotube array is an attractive architecture. The nanotube array could prolong the light penetration length in the axial direction, shorten the carrier collection distance in the radial direction and enlarge the semiconductor/liquid interface (SCLI).[9] Meanwhile, the nanotube array provides a strategy to enhance the light absorption through the anti-reflection effect.[9a] N-type α-Fe_2O_3 nanotubes have been fabricated through various template-based methods and anodization of Fe foil.[10] These α-Fe_2O_3 nanotubes exhibited appealing performances in gas sensing, Li-ion batteries and photoelectrochemical water oxidation.[10] However, few reports concern the fabrication of p-type α-Fe_2O_3 nanotubes, especially p-type α-Fe_2O_3 nanotube arrays. Here we report a facile anodic electrodeposition method to fabricate well-aligned nanotube arrays of p-type Zn-doped α-Fe_2O_3 on transparent conductive substrates. The electrodeposition method has the advantages of enhancing the electric contacts and minimizing the charge recombination at grain boundaries and other interfaces, which are beneficial for photoelectrodes.

The synthesis utilizes ZnO nanorod arrays on FTO-coated glass[11] as sacrificial templates and Zn sources, and 5 mM $FeCl_2$ aqueous solution (75 °C, pH = 4.0) as the electrolyte. An anodic potential of 1 V *vs.* saturated calomel electrode (SCE) was applied on the ZnO nanorod arrays for 5–15 min to enable the oxidation of the Fe^{2+} ions in the electrolyte to Fe^{3+} ions, which was followed by the precipitation of the Fe^{3+} ions as amorphous γ-FeOOH on the surface of the ZnO nanorods.[12] During this process, the ZnO nanorods were gradually dissolved by the acidic solution and anodic potential. After 2.5 min electrodeposition (ED), the ZnO nanorods completely dissolved, which is confirmed by the absence of the ZnO phase in the X-ray diffraction (XRD) spectrum (see Fig. S1, ESI†). Some of the Zn^{2+} ions dissolved in the electrolyte around the working electrode were *in situ* incorporated into γ-FeOOH. The deposits were annealed at 520 °C for 2 hours in the atmosphere, so as to convert the γ-FeOOH intermediates to α-Fe_2O_3 nanotubes.[12] The chemical reactions are provided in the ESI.†

The phase composition of samples in each step was analyzed by XRD. As shown in Fig. 1a, the XRD pattern of the ZnO nanorod arrays is consistent with that of wurtzite ZnO (JCPDS card no. 36-1451) with a preferential orientation in the ⟨001⟩ direction (the SEM image of the ZnO nanorods is provided in Fig. S2, ESI†). After 10 min electrodeposition, no diffraction peaks of ZnO were observed, confirming the complete dissolution of the ZnO nanorods. After the annealing process, the amorphous γ-FeOOH was converted

[a] *Key Laboratory of Photochemical Conversion and Optoelectronic Materials, Technical Institute of Physics and Chemistry, Chinese Academy of Sciences, Beijing, 100190, China. E-mail: shegw@mail.ipc.ac.cn, shiws@mail.ipc.ac.cn; Fax: +86-10-82543513; Tel: +86-10-82543513*

[b] *University of Chinese Academy of Sciences, Beijing, 100049, China*

† Electronic supplementary information (ESI) available: Experimental details; additional XRD, XPS and UV-Vis absorption spectrum of the Zn-doped α-Fe_2O_3 nanotubes; SEM image and photoelectrochemistry of the Zn-free α-Fe_2O_3 film. See DOI: 10.1039/c3cc40599k

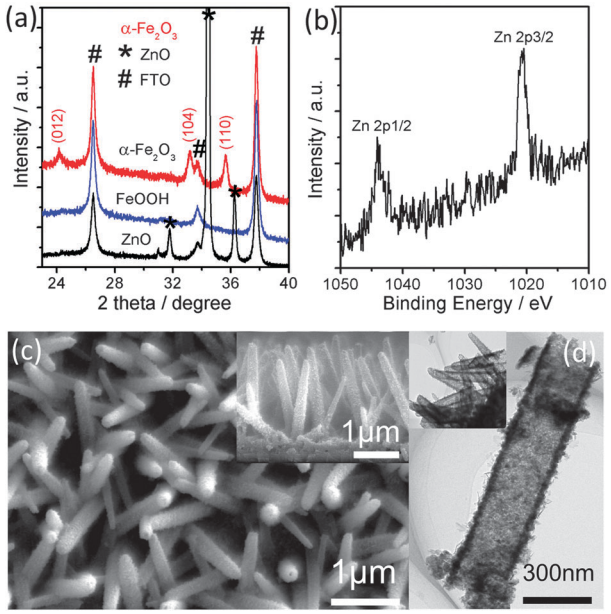

Fig. 1 (a) XRD patterns of the ZnO nanorods, Zn-doped FeOOH and Zn-doped α-Fe_2O_3 nanotubes; (b) XPS spectrum of Zn 2p in the Zn-doped α-Fe_2O_3 nanotubes; (c) SEM and (d) TEM images of the Zn-doped α-Fe_2O_3 nanotubes.

to α-Fe_2O_3 (hematite) with a rhombohedral structure (JCPDS card no. 86-0550). The presence of Zn in α-Fe_2O_3 was confirmed by the X-ray photoelectron spectroscopy (XPS) spectrum in Fig. 1b, in which the peaks at 1020.6 eV and 1044.1 eV can be indexed to Zn $2p_{3/2}$ and Zn $2p_{1/2}$, respectively. The atomic percentage of Zn in the surface of Zn-doped α-Fe_2O_3 (prepared with an ED time of 10 min) was determined to be 6.2 at% relative to Fe (the full range and Fe 2p XPS spectra can be seen in Fig. S3 and S4, ESI†). Fig. 1c shows the typical SEM images of α-Fe_2O_3, which closely replicates the morphologies of the ZnO nanorods (Fig. S2, ESI†) and exhibits a noticeable rough surface and slightly enlarged diameters. The TEM image in Fig. 1d clearly demonstrates the hollow structure of the Zn-doped α-Fe_2O_3 nanotubes. The formation of the nanotubes could also be observed from the high-resolution SEM images in Fig. S5 (ESI†). The mean wall thicknesses were identified to be 26(±5) nm, 36(±5) nm and 42(±5) nm for ED times of 5 min, 10 min and 15 min.

A three-electrode cell was used to investigate the photoelectrochemical properties of the Zn-doped α-Fe_2O_3 nanotubes. The linear scan voltammograms of the Zn-doped α-Fe_2O_3 nanotube arrays with an ED time of 10 min are shown in Fig. 2a. As can be seen, from 1.3 to 0.5 V *vs.* RHE (reversible hydrogen electrode), Zn-doped α-Fe_2O_3 shows a cathodic current increase upon illumination, which is the characteristic of a p-type semiconductor. By contrast, the Zn-free α-Fe_2O_3 film shows an anodic n-type photoresponse in the same potential region (see Fig. S6 and S7, ESI†), confirming that the p-type conductivity of Zn-doped α-Fe_2O_3 is caused by the Zn impurities, which serve as acceptors and induce the formation of the p-type α-Fe_2O_3.[6b] The photocurrent reaches 40.4 μA cm^{-2} at 0.5 V *vs.* RHE, which is much larger than that of a recently reported p-type α-Fe_2O_3 film prepared by atomic layer deposition and is comparable to that of the p-type Cu–Ti–O nanotube array.[2a,b] Further extending the potential to a more negative value than 0.5 V *vs.* RHE would cause an abrupt increase in both the dark current and the photocurrent.

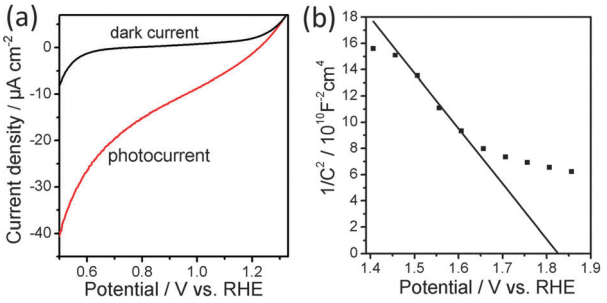

Fig. 2 (a) Linear sweep voltammograms of the Zn-doped α-Fe_2O_3 nanotubes prepared with an electrodeposition time of 10 min, in 1 M NaOH solution, under simulated AM 1.5G illumination of 100 mW cm^{-2}; (b) Mott–Schottky plot of the Zn-doped α-Fe_2O_3 nanotubes prepared with an electrodeposition time of 10 min, measured in the dark.

A similar phenomenon can also be observed on N-doped and Mg-doped p-type α-Fe_2O_3.[2a,6e] It may indicate that α-Fe_2O_3 is not stable at more negative potentials. Importantly, the Zn-doped α-Fe_2O_3 nanotubes exhibit a more positive photocurrent onset potential of 1.3 *vs.* RHE, which is several hundred mV more positive than those of some recently reported p-type semiconductors such as Mg-doped or N-doped α-Fe_2O_3, $CaFe_2O_4$, and Cu–Ti–O nanotube arrays.[2a–c,6e] For a photocathode, a more positive photocurrent onset potential suggests that more electric energy can be saved.[1] The excellent photoelectrochemical performance should be related to the efficient charge collection endowed by the nanotube-array architecture,[4a] in which the bulk recombination could be largely suppressed and the potential drop due to the charge transport in highly-resistant bulk α-Fe_2O_3 could also be minimized.

To further analyze the electronic properties of the α-Fe_2O_3 nanotubes, electrochemical impedance measurements were performed. The conducting type, dopant density and flatband potential of α-Fe_2O_3 can be calculated using the Mott–Schottky equation[1b]

$$1/C^2 = (2/e_0\varepsilon\varepsilon_0 N_a)[(V_{FB} - V) - kT/e_0]$$

wherein e_0 is the electron charge, ε is the dielectric constant of α-Fe_2O_3, ε_0 is the permittivity of vacuum, N_a is the dopant density, V is the electrode potential, V_{FB} is the flatband potential, T is the temperature and k is Boltzmann's constant. Fig. 2b shows a typical Mott–Schottky plot of the sample prepared with 10 min ED. The flat band potential of the Zn-doped α-Fe_2O_3 nanotubes was determined to be 1.82 V *vs.* RHE, which is much more positive than that of the Mg-doped hematite film.[2a] The positive flat band potential is of great importance to achieve the positive onset potential for the water reduction and to save the electric energy.[1b,c] The acceptor density in the present α-Fe_2O_3 nanotubes can be calculated from the equation

$$N_a = (2/e_0\varepsilon\varepsilon_0)[d(1/C^2)/dV]^{-1}$$

With an ε of 80, the acceptor density is calculated to be 4.19×10^{18} cm^{-3}, which is comparable to that of Zn-doped α-Fe_2O_3 prepared by spray pyrolysis deposition and is much larger than that of Mg-doped p-type α-Fe_2O_3.[2a,6b] The large acceptor density may be responsible for the excellent photoresponse observed for the as-prepared α-Fe_2O_3 nanotubes. For a band bending of $V - V_{FB} = 1$ V ($V = 0.82$ V *vs.* RHE), which is artificially selected

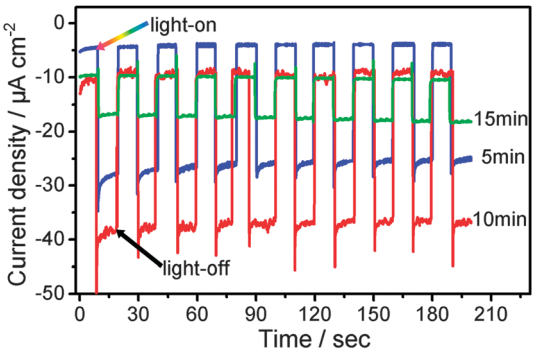

Fig. 3 Photoresponse of the Zn-doped α-Fe_2O_3 nanotube arrays prepared with ED times of 5 min, 10 min and 15 min, under chopped illumination, at a fixed potential of 0.5 V *vs.* RHE, in 1 M NaOH solution.

and reasonable for α-Fe_2O_3 with a bandgap of 1.9–2.2 eV, the acceptor density reveals a depletion layer width (W) of 45.9 nm, which can be determined from the equation

$$W = [2\varepsilon\varepsilon_0(V - V_{FB})/e_0N_a]^{1/2}$$

It should be noted that the wall thicknesses of the α-Fe_2O_3 nanotubes are less than the depletion layer width. It suggests that the electric field responsible for the charge separation exists over the entire α-Fe_2O_3. This would be very advantageous for the charge collection in α-Fe_2O_3, which has a short photogenerated carrier lifetime[8] and a short carrier diffusion length.[4]

The photoresponse of the samples prepared with different ED times are compared in Fig. 3. The reproducible photocurrents indicate that the α-Fe_2O_3 nanotubes are photoelectrochemically stable. The photocurrent increased when the ED time was prolonged from 5 min to 10 min. It could be attributed to the enhanced light absorption in the 10 min sample, which is confirmed by the UV-Vis absorption spectra in Fig. S8 (ESI†). Interestingly, when the ED time was further prolonged to 15 min, the photoresponse of the sample decreased dramatically. XPS analysis (Fig. S9, ESI†) shows that the atomic percentage of Zn in the surface of the α-Fe_2O_3 nanotubes decreased dramatically from 6.2 at% to 2.9 at% as the ED time was varied from 10 min to 15 min. The acceptor density, calculated from Mott–Schottky tests (see Fig. S10, ESI†), also decreased from 4.19×10^{18} cm^{-3} in the 10 min sample to 2.38×10^{18} cm^{-3} in the 15 min sample. This implies that there is a lightly Zn-doped layer at the outer part of the nanotube walls of the sample prepared in 15 min. Previous research indicates that the photoresponse of p-type α-Fe_2O_3 is very sensitive to the dopant density.[6c] This lightly-doped layer may be less conductive and could hinder the photogenerated charge carrier transfer from the bulk of α-Fe_2O_3 to the electrolyte. Thus, the 15 min sample exhibited smaller photocurrent than the 10 min sample despite the fact that it could absorb more incident light. The formation of this lightly doped layer could be rationalized by considering the concentration change of the Zn^{2+} ions in the electrolyte around the nanotubes during the electrodeposition process. The Zn^{2+} ions obtained from ZnO dissolution would diffuse from the nanotubes to the bulk electrolyte due to the concentration gradient. Thus, the concentration of Zn^{2+} ions around the nanotubes would gradually decrease with time. After long-time ED, the concentration of the Zn^{2+} ions around the nanotubes could be very low. Accordingly, a lightly-doped layer could be formed at the outer part of the nanotube walls. Efforts are still underway to enhance the dopant concentration in the α-Fe_2O_3 nanotubes.

In conclusion, we have reported an electrochemical method to synthesize p-type Zn-doped α-Fe_2O_3 nanotube arrays on transparent conductive substrates. A positive flat band potential of 1.82 V *vs.* RHE and an acceptor density of 4.19×10^{18} cm^{-3} were determined for the Zn-doped α-Fe_2O_3 nanotube arrays. The nanotube-array architecture facilitates the charge collection and the light absorption. These merits favor the Zn-doped α-Fe_2O_3 nanotubes with a positive photocurrent onset potential of 1.3 V *vs.* RHE and a cathodic photocurrent of 40.4 μA cm^{-2} at 0.5 V *vs.* RHE. The p-type α-Fe_2O_3 nanotube arrays are promising for construction of p–n junction photoelectrodes and tandem devices for overall water splitting.

This work was financially supported by the Chinese Academy of Sciences, NSFC (grant no. 21103211, 50902134, 51272258, 51272302 and 61025003), and the National Basic Research Program of China (973 Program) (grant no. 2010CB934103).

Notes and references

1 (*a*) A. J. Bard, *J. Phys. Chem.*, 1982, **86**, 172; (*b*) A. J. Nozik and R. Memming, *J. Phys. Chem.*, 1996, **100**, 13061; (*c*) M. G. Walter, E. L. Warren, J. R. McKone, S. W. Boettcher, Q. Mi, E. A. Santori and N. S. Lewis, *Chem. Rev.*, 2010, **110**, 6446.
2 (*a*) Y. Lin, Y. Xu, M. T. Mayer, Z. I. Simpson, G. McMahon, S. Zhou and D. Wang, *J. Am. Chem. Soc.*, 2012, **134**, 5508; (*b*) G. K. Mor, O. K. Varghese, R. H. T. Wilke, S. Sharma, K. Shankar, T. J. Latempa, K. S. Choi and C. A. Grimes, *Nano Lett.*, 2008, **8**, 1906; (*c*) S. Ida, K. Yamada, T. Matsunaga, H. Hagiwara, Y. Matsumoto and T. Ishihara, *J. Am. Chem. Soc.*, 2010, **132**, 17343; (*d*) W. B. Ingler and S. U. M. Khan, *Electrochem. Solid-State Lett.*, 2006, **9**, G144; (*e*) C. Leygraf, M. Hendewerk and G. A. Somorjal, *J. Phys. Chem.*, 1982, **86**, 4484.
3 (*a*) A. Paracchino, V. Laporte, K. Sivula, M. Graetzel and E. Thimsen, *Nat. Mater.*, 2011, **10**, 456; (*b*) M. H. Lee, K. Takei, J. Zhang, R. Kapadia, M. Zheng, Y. Z. Chen, J. Nah, T. S. Matthews, Y. L. Chueh, J. W. Ager and A. Javey, *Angew. Chem., Int. Ed.*, 2012, **51**, 10760; (*c*) B. Seger, A. B. Laursen, P. C. K. Vesborg, T. Pedersen, O. Hansen, S. Dahl and I. Chorkendorff, *Angew. Chem., Int. Ed.*, 2012, **51**, 9128.
4 (*a*) K. Sivula, F. Le Formal and M. Graetzel, *ChemSusChem*, 2011, **4**, 432; (*b*) Y. Lin, G. Yuan, S. Sheehan, S. Zhou and D. Wang, *Energy Environ. Sci.*, 2011, **4**, 4862.
5 Y. Ling, G. Wang, J. Reddy, C. Wang, J. Z. Zhang and Y. Li, *Angew. Chem., Int. Ed.*, 2012, **51**, 4074.
6 (*a*) J. E. Turner, M. Hendewerk, J. Parmeter, D. Neiman and G. A. Somorjai, *J. Electrochem. Soc.*, 1984, **131**, 1777; (*b*) W. B. Ingler, J. P. Baltrus and S. U. M. Khan, *J. Am. Chem. Soc.*, 2004, **126**, 10238; (*c*) W. B. Ingler and S. U. M. Khan, *Thin Solid Films*, 2004, **461**, 301; (*d*) W. B. Ingler and S. U. M. Khan, *Int. J. Hydrogen Energy*, 2005, **30**, 821; (*e*) T. Morikawa, K. Kitazumi, N. Takahashi, T. Arai and T. Kajino, *Appl. Phys. Lett.*, 2011, **98**, 242108.
7 P. Liao, M. C. Toroker and E. A. Carter, *Nano Lett.*, 2011, **11**, 1775.
8 S. R. Pendlebury, M. Barroso, A. J. Cowan, K. Sivula, J. Tang, M. Graetzel, D. Klug and J. R. Durrant, *Chem. Commun.*, 2011, **47**, 716.
9 (*a*) X. Qi, G. She, Y. Liu, L. Mu and W. Shi, *Chem. Commun.*, 2012, **48**, 242; (*b*) G. K. Mor, H. E. Prakasam, O. K. Varghese, K. Shankar and C. A. Grimes, *Nano Lett.*, 2007, **7**, 2356; (*c*) N. Chouhan, C. L. Yeh, S. F. Hu, R. S. Liu, W. S. Chang and K. H. Chen, *Chem. Commun.*, 2011, **47**, 3493.
10 (*a*) N. Kang, J. H. Park, J. Choi, J. Jin, J. Chun, I. G. Jung, J. Jeong, J. G. Park, S. M. Lee, H. J. Kim and S. U. Son, *Angew. Chem., Int. Ed.*, 2012, **51**, 6626; (*b*) J. Chen, L. N. Xu, W. Y. Li and X. L. Gou, *Adv. Mater.*, 2005, **17**, 582; (*c*) S. K. Mohapatra, S. E. John, S. Banerjee and M. Misra, *Chem. Mater.*, 2009, **21**, 3048; (*d*) Z. Wang, D. Luan, S. Madhavi, C. M. Li and X. W. Lou, *Chem. Commun.*, 2011, **47**, 8061; (*e*) X. Qu, N. Kobayashi and T. Komatsu, *ACS Nano*, 2010, **4**, 1732.
11 (*a*) G. She, X. Zhang, W. Shi, X. Fan, J. Chang, C. Lee, S. Lee and C. Liu, *Appl. Phys. Lett.*, 2008, **92**, 053111; (*b*) G. She, X. Zhang, W. Shi, X. Fan and J. Chang, *Electrochem. Commun.*, 2007, **9**, 2784.
12 R. L. Spray and K. S. Choi, *Chem. Mater.*, 2009, **21**, 3701.

